

Chemical, Petroleum and Environmental Engineering

Synthesis and Characterization of Nanocrystalline Aluminophosphate AlPO₄-5 Molecular Sieve

Asir Alnaama

Instructor Dr. , Consultant in Student Affairs Dept., lecturer in Chem.Eng. Dept.,
Engineering college-Baghdad University
Email:dr.asir.alnaama@gmail.com

ABSTRACT

Nanocrystalline aluminophosphate AlPO₄-5 molecular sieves were synthesized by hydrothermal method (HTS). Synthesis parameters like time and temperature of crystallization were investigated. Type of template (R) and ratio of R/P₂O₅ were studied also. Characterization of the synthesized AlPO₄-5 were done by powder X-ray diffraction (XRD), scanning electron microscopy (SEM/EDX), Fourier transform infrared (FTIR), differential scanning calorimetry-thermogravimetry analysis (DSC-TGA), and N₂ adsorption-desorption BET analysis. XRD patterns results showed excellent crystallinity for two types of templates, di-n-propylamine (DPA) and tetrapropyl ammonium hydroxide (TPAOH) for aluminophosphate five (AFI) structure. Nano-level for particle size of 66 nm was revealed by AFM test. Good thermal stability was obtained in DSC-TGA results. Best time and temperature of crystallization of 24h and 190 °C were got. Optimum R/P₂O₅ for two kind of template was established.

Keywords: Aluminophosphate, AFI, AlPO₄-5, Molecular sieves, Nanocrystalline.

1. INTRODUCTION

Aluminophosphate (AlPO₄) molecular sieves have drawn the attention of the researchers and extensively investigated due to their excellent properties. Similar to, zeolite AlPO₄ molecular sieves are constructed by phosphorous and aluminum tetrahedral. Their metal substituted (isomorphously) molecular sieves have many applications in catalysis and catalytic reactions like isomerization and others, **Rajesh, et al., 2001, Hartmann and Elangovan, 2003, Choi, et al., 2006, Wekhysen, et al., 1991, Wang, et al., 2009, and Li, et al., 2004.**

The novel structure of aluminophosphate (AlPO₄) based molecular sieves showed a variety in pore size and can be classified to large pore (0.7-0.8nm) like AlPO₄-5 (AFI-aluminophosphate five structure), intermediate pore (0.6nm) like AlPO₄-11 (AEL-aluminophosphate eleven structure), small pore (0.4nm) like AlPO₄-14 (AFN-Aluminophosphate fourteen structure), **Rajesh, et al., 2001.**

The framework of AlPO₄-5 (AFI) is hexagonal with a=1.373 nm, c=0.848 nm and consists of columns of twisted 4- and 6- rings parallel to c-axis giving a unidimensional 12-rings and free diameter of pore 0.73 nm. The framework of AlPO₄-11(AEL) is generated by elimination of



one-third of the rings from $\text{AlPO}_4\text{-5}$ framework and conversion of each 12-ring rounded channel into an elliptical 10-ring channel with diameter of 0.67nm by 0.40nm, by The templates used in incorporation into channel during synthesis are di-n-propylamine (DPA) for $\text{AlPO}_4\text{-5}$ and tetrapropyl ammonium forming $\text{AlPO}_4\text{-11}$, **Flanigen, et al., 1986**.

AlPO_4 molecular sieves exhibit excellent thermal and hydrothermal stability comparable to zeolites. The frameworks of AlPO_4 's are neutral and exhibit weakly acidic catalytic properties, so isomorphous incorporation of metals is essential for improving the catalytic performance of AlPO_4 's.

Synthesis of AlPO_4 were investigated using different techniques mostly by hydrothermal (Solvothermal) synthesis (HTS), **Gielgens, et al., 1995, Hassanvan and Ashgari, 2012, Wan, et al., 2000, Klap, et al., 1999, Zhang, 2013, and Naydenov, 2003**, and recently by ionothermal synthesis using ionic liquid solution (ILS), **Wei, et al., 2010, Fayad, et al., 2010, Han, et al., 2007, Xu, et al., 2006, and Sun, 2012s**.

Li, et al., 2012, investigated the effect of precursor gel preparation on the microstructure of aluminophosphate $\text{AlPO}_4\text{-5}$ in the hydrothermal synthesis. They studied synthesis of $\text{AlPO}_4\text{-5}$ via two different route, one-off addition (acid and template) without stirring and no stirring in the overnight aging process (Route 1), and dropwise addition of reagents with stirring and continuous stirring in the overnight aging process (Route 2).They concluded that the gel preparation by route 2 is likely affects early crystallization more than prolonged crystallization.

Khoo, et al., 2012, investigated the synthesis of AlPO_4 by ionothermal synthesis using 1-ethyl-2,3 dimethylimidazolium bromide ([edmim]Br) ionic liquid (IL) as both solvent and structure directing agent (SDA), they found that crystallinity, size of the $\text{AlPO}_4\text{-5}$ to be strongly affected by chemical composition of the gel solution and heating time of the gel mixture.

Wan, et al., 2004, investigated the role of water content in the hydrothermal synthesis and characteristics of $\text{AlPO}_4\text{-5}$ samples, they concluded that when $\text{AlPO}_4\text{-5}$ samples are synthesized from molar gel compositions with 10 or $20\text{H}_2\text{O}$ there is preference for the formation of thin hexagonal platelets, and when the gel composition with 30 or $40\text{H}_2\text{O}$, the preferred morphology are spheres.

In this research work $\text{AlPO}_4\text{-5}$ (AFI) investigated using tetrapropyl ammonium hydroxide (TPAOH) and di-n-propylamine (DPA) as template, aluminum isopropoxide (AIP) and phosphoric acid as structural element sources, with hydrothermal synthesis using autoclave as described previously in, **Alnaama, 2015**.

2. EXPERIMENTAL

2.1 Materials

Phosphoric acid (85 wt.%, Merck) and aluminum isopropoxide (AIP, sigma Aldrich) were used as phosphor and alumina sources respectively, tetrapropyl ammonium hydroxide (TPAOH-Wuhan kemi chemical-chinese) and di-n-propylamine (Merck) as template (R), and deionized water.



2.2 Synthesis methods

Aluminum isopropoxide (AIP) 5 g was mixed with 45 ml deionized water and stirred for 30 min. Phosphoric acid (85%) 5.65 g was added to the solution of AIP by dropwise method in 30 min period of time. Different amounts of template (R) tetrapropyl ammonium hydroxide (TPAOH) or di-n-propylamine (DPA) were added to the solution and stirred for 2h. the gel solution was transferred into the autoclave and operated at 190°C temperature for 24h. Then the autoclave was cooled and the sample product washed, filtered, and dried overnight at 100°C in oven. The dried samples then calcined for 5h at 550°C.

2.3 Characterization Techniques

The crystalline phase of the samples was determined by X-ray diffraction (XRD) (PHASER/Bruker, Germany, 2010), with Ni-filtered $\text{CuK}\alpha$ radiation with $\lambda = 1.54 \text{ \AA}$ (30 Kv, 10 mA) with a $0.02^\circ 2\theta$ step and 0.5 s per step. XRD includes also the analysis of Scherer for crystallite size for each peak.

Fourier transform infrared (FTIR) spectrum was carried using sample diluted in KBr (1% in 99% KBr) and analyzed by IR-Prestige-21 (Shimadzu).

Scanning electron microscopy (SEM/EDX) for the morphology were conducted by Inspect S50 including energy dispersive XRD (EDX) , FEI (USA). DSC-TGA was analyzed by Linseis Model STA PT-1000 (Germany) with sample weight 20 mg and temperature ramp 10°C .

3. RESULTS AND DISCUSSION

3.1 Characterization

3.1.1 XRD

Analysis of XRD pattern showed that peaks positions for the AFI structure was obtained, with 95% crystallinity for $\text{AlPO}_4\text{-5}$ (M9) and as shown in **Table 2** and **Fig. 1**, when comparing the peak positions (2θ), space distance (d_s) with theoretical value stated in, **Meier, et al., 1996**, showed excellent agreement.

3.1.2 SEM/EDX

Energy dispersive X-ray was tested and as shown in **Fig. 5** for elemental analysis. Morphology of $\text{AlPO}_4\text{-5}$ (AFI) was investigated by SEM as shown in **Fig. 6**. The electronic images revealed a highly crystalline aggregates of crystals and formation of microparticles caused by agglomeration of nanoparticles, which in turn can lead to mesoporosity created by interparticles voids, the creation of these voids are as consequence of agglomeration besides some defects may appear in crystals formation.

3.1.3 Atomic Force Microscopy (AFM)

Fig. 7 and **8** showed the AFM images for samples 9M and 11M respectively, the images revealed the detailed observation of nano-scale events at crystal surface, showing also the height of terraces and layer of growth. These observations are well agreed with the work of **Aghabozog, et al., 2012**.



Average particle size of 66.5 nm obtained for sample M11 and 84.9 nm for M9. This result is confirmed, by comparing the crystallite size calculated by Scherer analysis through the measurement of FWHM (the broadening of the peaks) in XRD pattern, which gave an average of 23.5, 39.8 and 46.2 nm for samples M9, M10, and M11 respectively for crystallite size analyzed by scherer analysis through XRD pattern and as shown in **Table 3** below.

3.1.4 BET Analysis

The results of BET surface area is as shown in **Fig. 9** for isotherm plot for $\text{AlPO}_4\text{-5}$ (sample M9), where quantity adsorbed is plotted versus relative pressure p/p_0 , in which the adsorption-desorption curve reveals a hysteresis loop that means it has little porosity. BET surface is $185 \text{ m}^2/\text{g}$ and pore volume is $0.153 \text{ cm}^3/\text{g}$, these results are in agreements with reported results in **MacIntosh, 2012**.

3.1.5 Fourier transform Infrared (FTIR)

FTIR spectrum for produced sample is shown in **Fig. 16**, the results are well agree with reported data in, **Rajesh, et al., 2001, Khoo, et al., 2013, Zhu, et al., 2001**.

The details of bands located in the spectrum are summarized in **Table 3** below, and T-O-T represent Al-O-P. The location of asymmetric and symmetric stretching bands and bending band were mentioned.

3.1.6 DSC-TGA

DSC-TGA result of sample $\text{AlPO}_4\text{-5}$ (M9), revealed that the synthesized and calcined product is thermally stable and showed that there is no occluded water and/or template in product as shown in **Fig. 11**.

3.2 Effect of Synthesis parameters

3.2.1 Temperature of Crystallization

Crystallization temperature of 180°C and 190°C were experienced and revealed that good crystallization can be obtained at 180°C , meantime at 190°C besides good crystallization, it gave best results towards decreasing particle size (66.5 nm). The effect of increasing temperature of crystallization were also concluded by **Alnaama, 2012** in synthesis of aluminosilicate (zeolites), and **Zhu, et al., 2001**, in synthesis of aluminophosphates indicating a behavior similarity in effect of crystallization temperature for both types of molecular sieves in obtaining nanocrystalline molecular sieves. **MacIntosh, 2012**, investigated crystallization of aluminophosphate molecular sieves family and concluded that they have few subtle differences in crystallization from zeolites, and the reaction of aluminum oxide with phosphoric acid to form amorphous aluminophosphate and the solid phase rearranges as the crystallization proceeds more rapidly as temperature increases.

3.2.2 Template

Type of template and ratio of template to phosphoric pentoxide ($\text{R/P}_2\text{O}_5$) found to have vital role in getting good crystallinity and nanocrystalline powder. The choice for the value of this



ratio were carefully studied through the literature survey besides considering the technical procedures used in samples preparations and syntheses. TPAOH used with molar ratio of 1.0 (TPAOH/P₂O₅) gave, in AFM test, average particle size of 66 nm. While DPA gave 84 nm in molar ratio (DPA/P₂O₅) of 1.8. This difference in molar ratio can be explained by the difference in size of template molecule, for larger molecule as in TPAOH needs less molar ratio, but for smaller one DPA needs more molar ratio to occupy the inside void in the structure, in other words, the size of template molecule play a major role in occupying the necessary volume inside the pore volume of structure, so as TPAOH molecule is bigger than DPA molecule so it needs less no. of moles to give the same results in structuring the molecular sieve.

4. CONCLUSIONS

The concluded notes of this research can be summarized as following:

- Nanocrystalline aluminophosphate AlPO₄-5 (AFI) molecular sieves can be synthesized by hydrothermal (solvothetical) reaction method with optimum ratio of R/P₂O₅ at specified time and temperature of crystallization.
- Both templates TPAOH and DPA gave nano-scale particle size results at optimum ratio of R/P₂O₅ where it was 1.8 for DPA and 1.0 for TPAOH.
- Temperature of crystallization has vital role on getting nano-scale for particle size.

ACKNOWLEDGMENT

The Author express his thanks for college of pure science-ibnalhaytham for DSC-TGA. College of Science, Univ. of Baghdad for conducting XRD and AFM. College of science-Univ. of Alnahrain for SEM and EDX. Ibn Sina laboratory for FTIR.

5. REFERENCES

- B.Rajesh, M.Palanichamy, V.Murugesan, 2001, *Mesoporous Aluminophosphate and silicoaluminophosphate Molecular Sieves:Room Temperature Synthesis, Characterization, and Catalytic Performance*, Indian journal of Chemistry, Vol.40A, pp1262-1268.
- M.Hartmann, S.P.Elangovan,2003, *Isomerization and Hydrocracking of n-decane over Magnesium-containing Molecular Sieves with AEL, AFI, and AFO Topology*, Wiley on line, Vol.26, issue 12, pp.1232-1235.
- M.Choi, R.Srivastra, R.Ryoo,2006, *Organosilane Surfactant-Directed Synthesis of Mesoporous Aluminophosphate Constructed with Crystalline Microporous Frameworks*, J. Chem. Comm., issue 42, pp.4380-4388.
- B.M. Weckhuysen, R.R.Rao, J.A.Martens, R.A.Schoonheydet,1999, *Transition Metal Ions in Microporous Crystalline Aluminophosphate:Isomorphous Substitution*, Eur.J. of Inorg.Chem.,pp.565-577.
- Q.Wang, G.Chen, S.Xu, 2009, *Hierarchical Architecture Observed in Microspheres Comprising AlPO₄-11 Nanocrystals*, J.Micropor.Mesopor.Mater., Vol.119, pp.315-321.
- J.J.Li, G.D.Li, C.Y.Xi, Y.Guo, J.S.Chen, 2004, *Synthesis and Characterization of AlPO₄ and MAPO-11 Single Crystal*, Chem.Res.Chinese, Vol.20, No.2, pp. 131-133.



- E.M.Flanigen, B.M.Lok, R.L.Patton, S.T.Wilson, 1986, *Aluminophosphate Molecular Sieves and the Periodic Table*, J. Pure & appl.Chem., Vol.58, No.10, pp 1351-1358.
- L.H.Gielgens, I.H.E.Veenstra, V.Ponee, M.J. Haanepen, J.H.C. Van Hoof, 1995, *Selective Isomerization of n-butene by Crystalline Aluminophosphates*, J. Catalysis Letters, Vol.32, pp 195-203.
- -A.Hassanvan, M.Asghari, 2012, *Fabrication and Characterization of AlPO₄-5 Nanozeolite: Effect of Hydrothermal Temperature and Duration*, J.of Ceramic processing Research, Vol.13, No.1, pp 56-68.
- Y.Wan, C.D.Williams, C.V.A.Duke, J.J.Cox, 2000, *Systematic Studies on the Effect of Water Content on the Synthesis, Crystallization, Conversion, and Morphology of AlPO₄-5 Molecular Sieve*, J.of Materials Chemistry, Vol.10, pp2857-2862.
- G.L.Klap, M.Wubbenhorst, J.C.Jansen, H.Van Koningsveld, H.Van Bekkum, J.Van Turnhout, 1999, *polar Growth and Directional Adsorption of large AlPO₄-5 Crystals Determined by Scanning Pyroelectric Microscopy*, J.of Chemistry Letters, Vol.11, pp 3497-3503.
- L.Zhang, 2013, *Investigation of the Crystallization Process of Molecular Sieves*, Ph.D. Thesis, School of Graduate and Postdoctoral Studies, University of Western Ontario, Canada
- V.Naydenov, 2003, *Structured Molecular Sieves: Synthesis, Modification and Characterization*, Ph.D. Thesis, Department of Chemical and Metallurgical Engineering, division of Chemical Technology, Lulea university of technology.
- Y.We, Z.Tian, H.Gies, R.Xu, H.Ma, R.Pie, W.Zhang, Y.Xu, L.Wang, K.Li, B.Wang, G.Wen, L.Lin, 2010, *Ionothermal Synthesis of an aluminophosphate Molecular Sieve with 20-ring Pore Opening*, Angew.Chem.,Vol.122, pp 5495-5498.
- E.J.Fayad, N.Bats, C.E.A.Kirschhock, B.Rebours, A.A.Quineaud, J.A.Martens, 2010, *A Rational Approach to the Ionothermal Synthesis of an AlPO₄ Molecular Sieve with an LTA-Type Framework*, Angew.chem., pp 4689-4692.
- L.Han, Y.Wang, C.Li, S.Zhang, X.Lu, M.Cao, 2007, *Simple and Safe Synthesis of Microporous Aluminophosphate Molecular Sieves by Ionothermal Approach*, J.AICHE, Vol.54, No.1, pp 280-287.
- Y.P.Xu, Z.J.Tian, S.J.Wang, Y.Mu, L.Wang, B.C.Wang, Y.C.Ma, L.Hou, J.Y.Yu, L.W.Lin, 2006, *microwave-Enhanced Ionothermal Synthesis of Aluminophosphate Molecular Sieves*, Angewchem.Int.Ed., Vol.45, pp 3965-3970.
- X.Sun, 2012, *Fundamental Research of the Solvent Role in the Ionothermal Synthesis of Microporous Materials*, Ph.D. Dissertation, Dept. of Chem. Eng., Kansas State Univ., USA.
- D.Li, J.F.Yao, H.Wang, 2012, *Hydrothermal Synthesis of AlPO₄-5: Effect of Precursor Gel Preparation on the Morphology of Crystals*, J. Progress in Natural Science: Materials International, Vol.22, Issue 6, pp.684-692.
- D.Y.Khoo, W.M.Kok, R.R.Mukti, S.Mintova, E.P.Ng, 2013, *Ionothermal Approach for Synthesizing AlPO₄-5 with Hexagonal Thin-Plate Morphology influenced by Various parameters at Ambient Pressure*, J. of Solid State Science, Vol.25, pp 63-69.



- Y.Wan, D.Craig, C.V.A.Duke, J.C.Jeff, 2004, *Systematic Studies on the Effect of Water Content on the Synthesis, Crystallization, Conversion and Morphology of AlPO₄ Molecular Sieves*, J. of Materials Chemistry, Vol.10, pp 2857-2862.
- A.A.Alnaama, 2015, *Synthesis and Characterization of Nanocrystalline ZSM-5 and ZSM-5/MCM-41 Composite Zeolite for Biodiesel Production*, Ph.D. Thesis, Chem. Eng. Dept., College of Eng., Univ. of Baghdad.
- W.M.Meier, D.H.Olson, C.H. Baerlocher, 1996, *Atlas of Zeolite Structure Types*, 4th ed., Elsevier, Amestrdam.
- H.Aghabozog, S.Hassani, F.Salehirad, 2012, *Crystal growth Study of Nano-zeolite by Atomic Force Microscopy In: N.Kolesnikov, ed. Modern Aspects of Bulk Crystal and Thin Film Preparation*, S.1.:S.n, pp 357-372.
- G.Zhu, S.Qui, F.Gao, G.Wu, R.Wang, B.Li, Q.Fang, Y.Li, B.Gao, Y.Li, X.Xu, O.Terasaki, 2001, *Synthesis of Aluminophosphate Molecular Sieve AlPO₄-11 Nanocrystals*, Micropor. Mesopor. Mater., Vol.50, pp.129-135.
- A.R.MacIntosh, 2012, *Studies on Molecular Sieve Crystallzation and Heteroatomic Substitution*, M.Sc. Thesis, Univ. of Western Ontario, Canada.

Table 1. Molar Composition of Samples.

Sample	Molar composition
M9	1.8R ₁ .Al ₂ O ₃ .P ₂ O ₅ .102H ₂ O
M10	1.2R ₁ .Al ₂ O ₃ .P ₂ O ₅ .102H ₂ O
M11	1.0R ₂ .Al ₂ O ₃ .P ₂ O ₅ .102H ₂ O

Where R₁=DPA (*di-n-propylamine*)

R₂=TPAOH (*tetrapropyl ammonium hydroxide*)

Table 2. XRD Data for sample M9 compared with theoretical values.

hkl	2θ	ds,Å	I _{rel} s
100	7.401(7.43)	11.9346(11.899)	100(100)
110	12.82(12.89)	6.8958(6.870)	20.2(6.3)
200	14.84(14.89)	5.9632(5.950)	9.1(20.6)
210	19.679(19.74)	4.5075(4.497)	28.1(42.4)
002	20.37(20.97)	4.3561(4.237)	13.4(45.3)
102	22.37(22.27)	3.9708(3.992)	37.2(12.5)
220	25.833(25.94)	3.4459(3.435)	13.4(19.6)

The values between parenthesis represents the theoretical values abstracted from, **Meier, et al., 1996.**

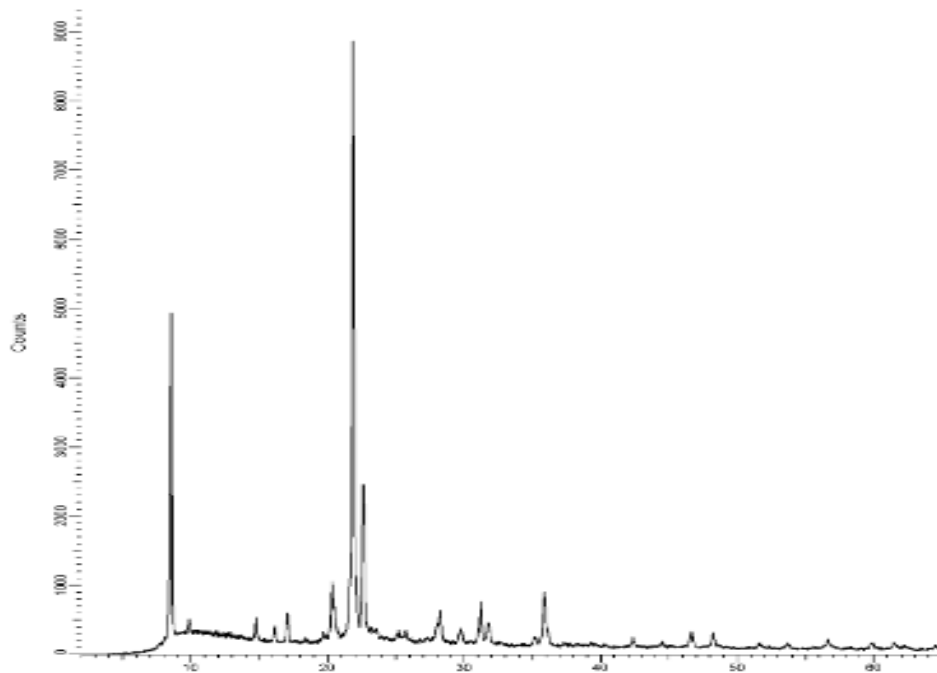


Figure 1. XRD for M9.

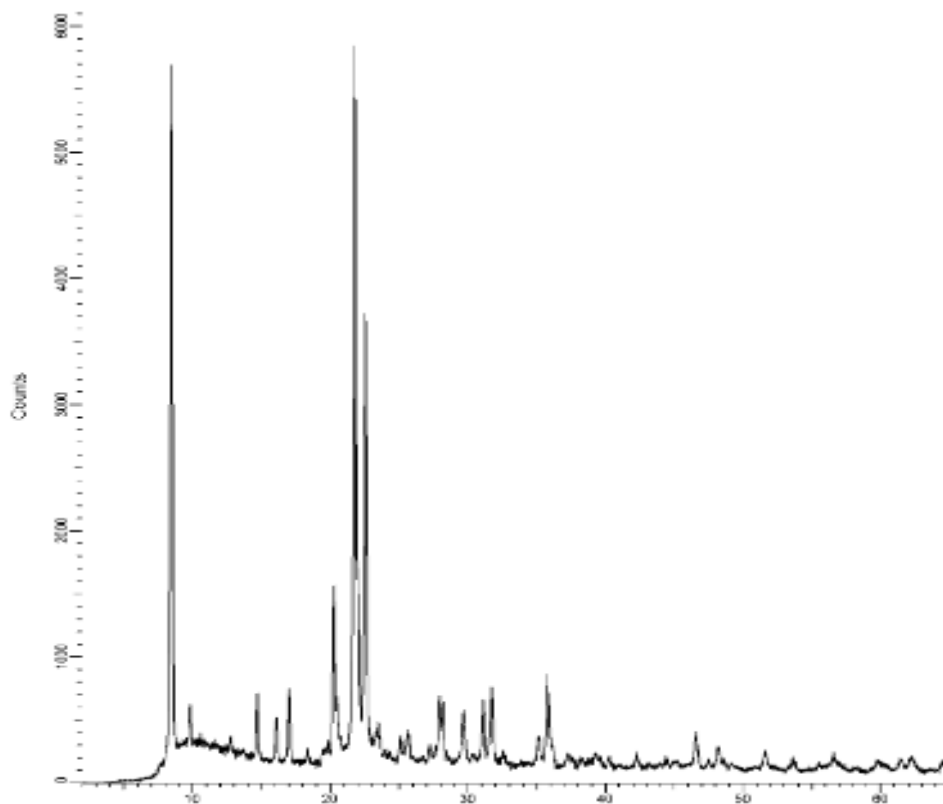


Figure 2. XRD for M10.

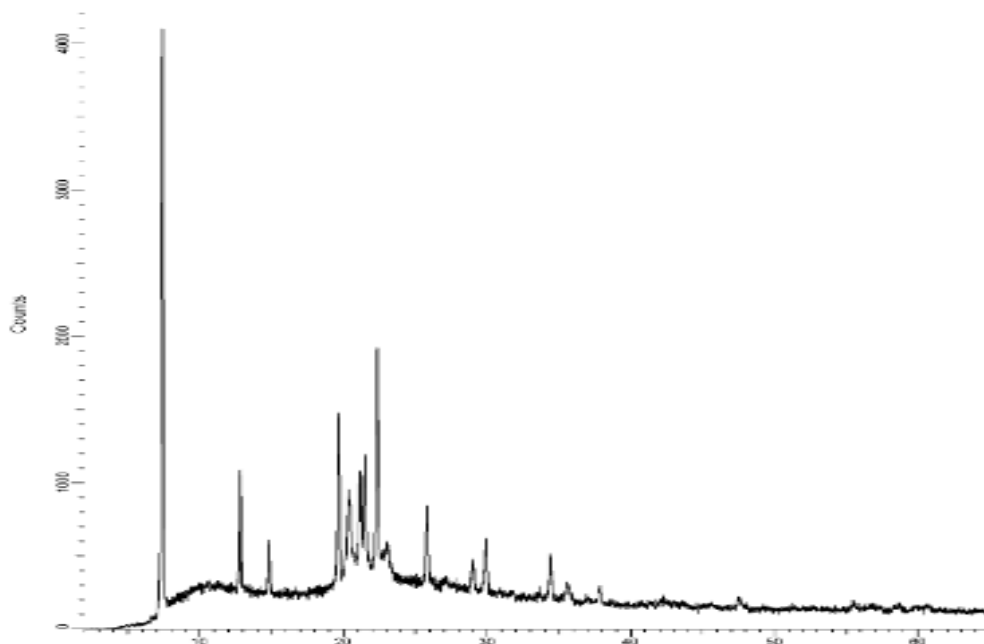


Figure 3. XRD for M11.

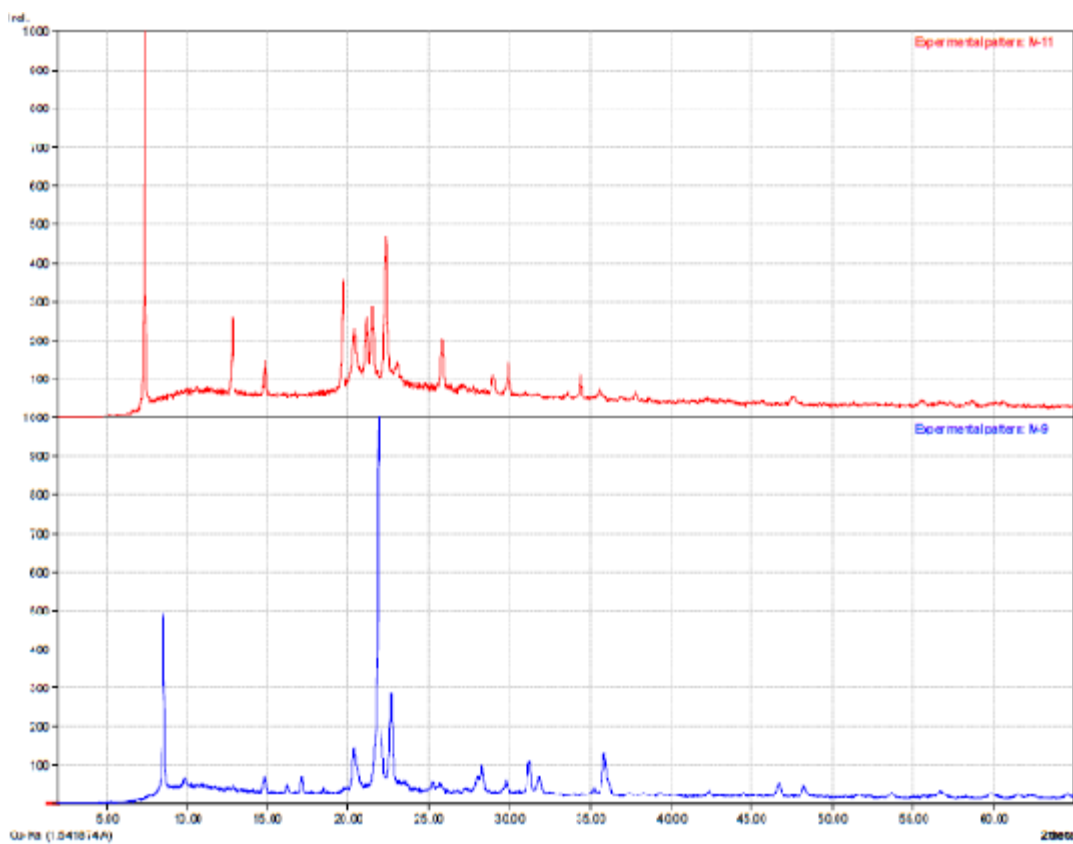


Figure 4. XRD for M9 and M11.

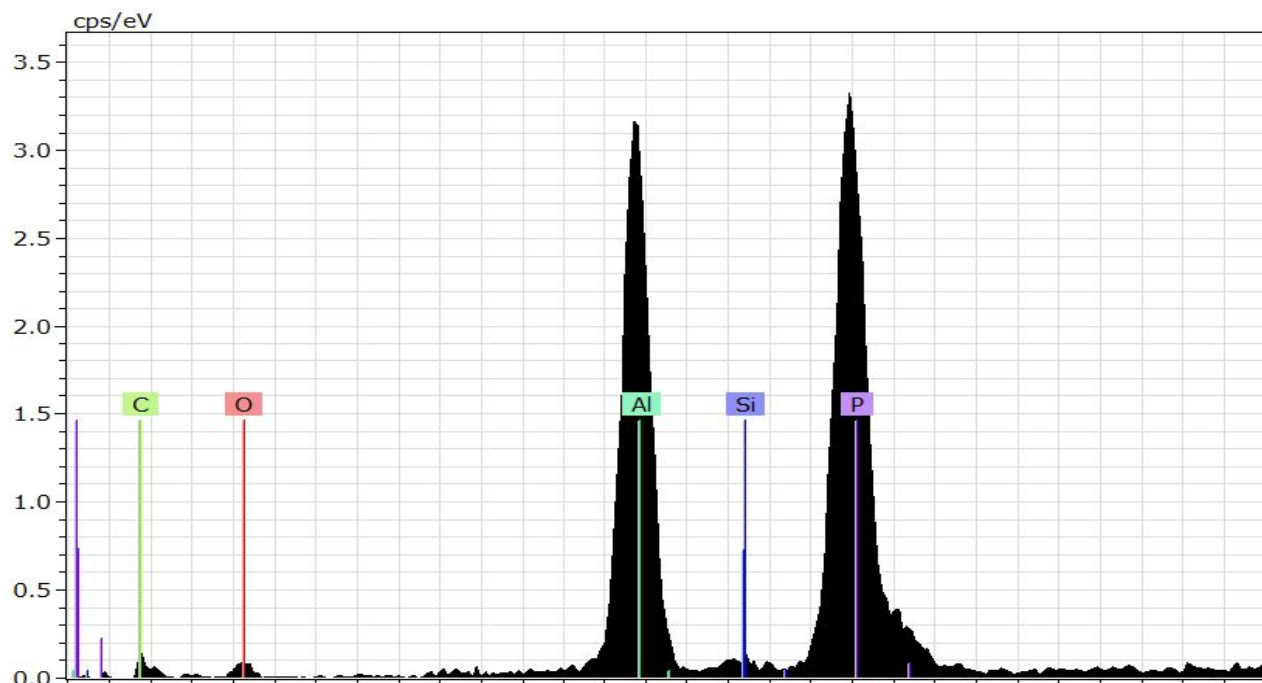


Figure 5. EDX for M9.

Table 3. Particle size and Crystallite size.

	Sherer Crystallite size range,nm	Scherer Ave. Crystallite size, nm	AFM particle size,nm
M9	10.8-60.4	23.5	84.9
M10	9.5-100	39.8	32.1
M11	13.2-100	46.2	66.5

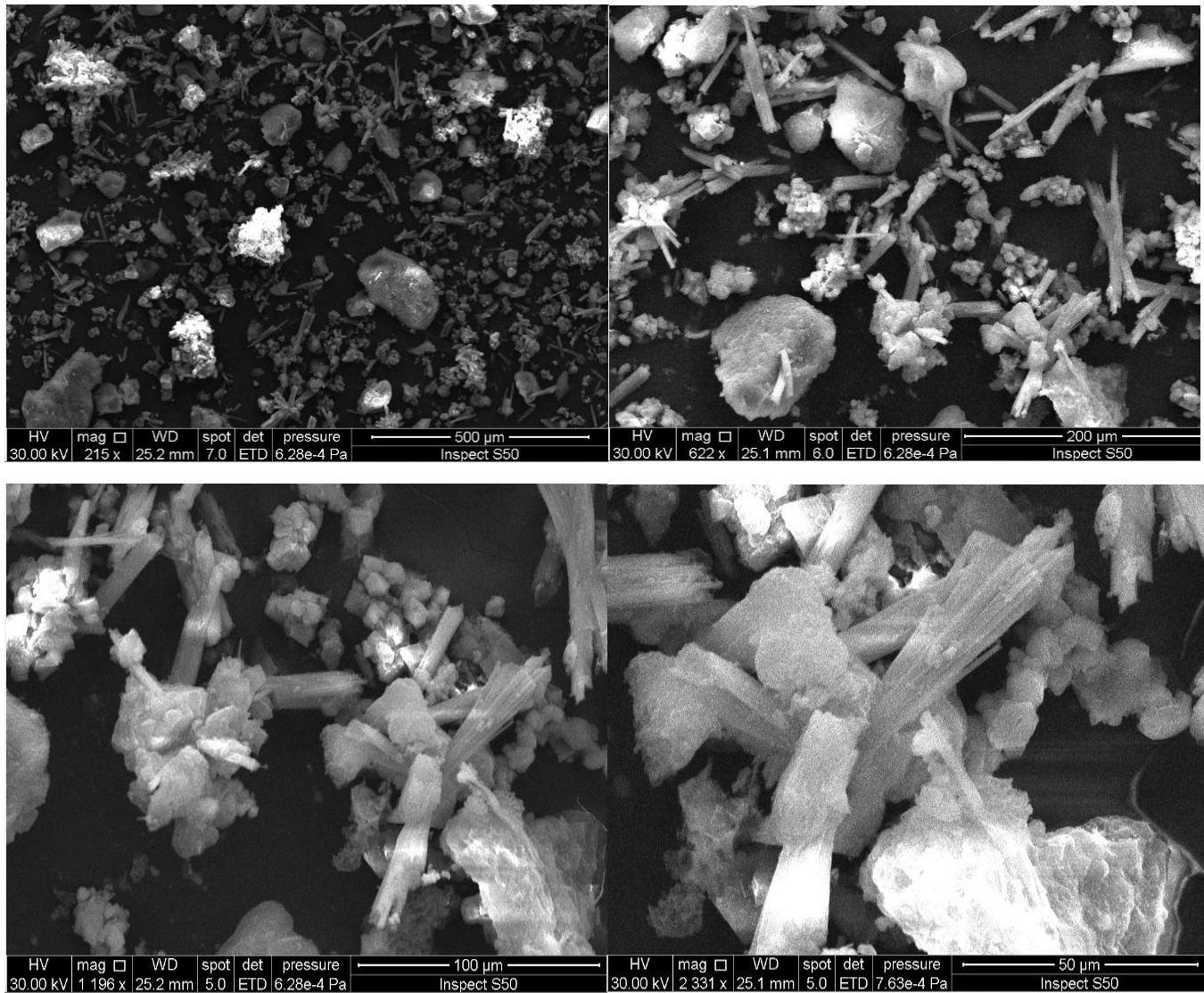


Figure 6. SEM Images for AlPO₄-5 (sample M9).

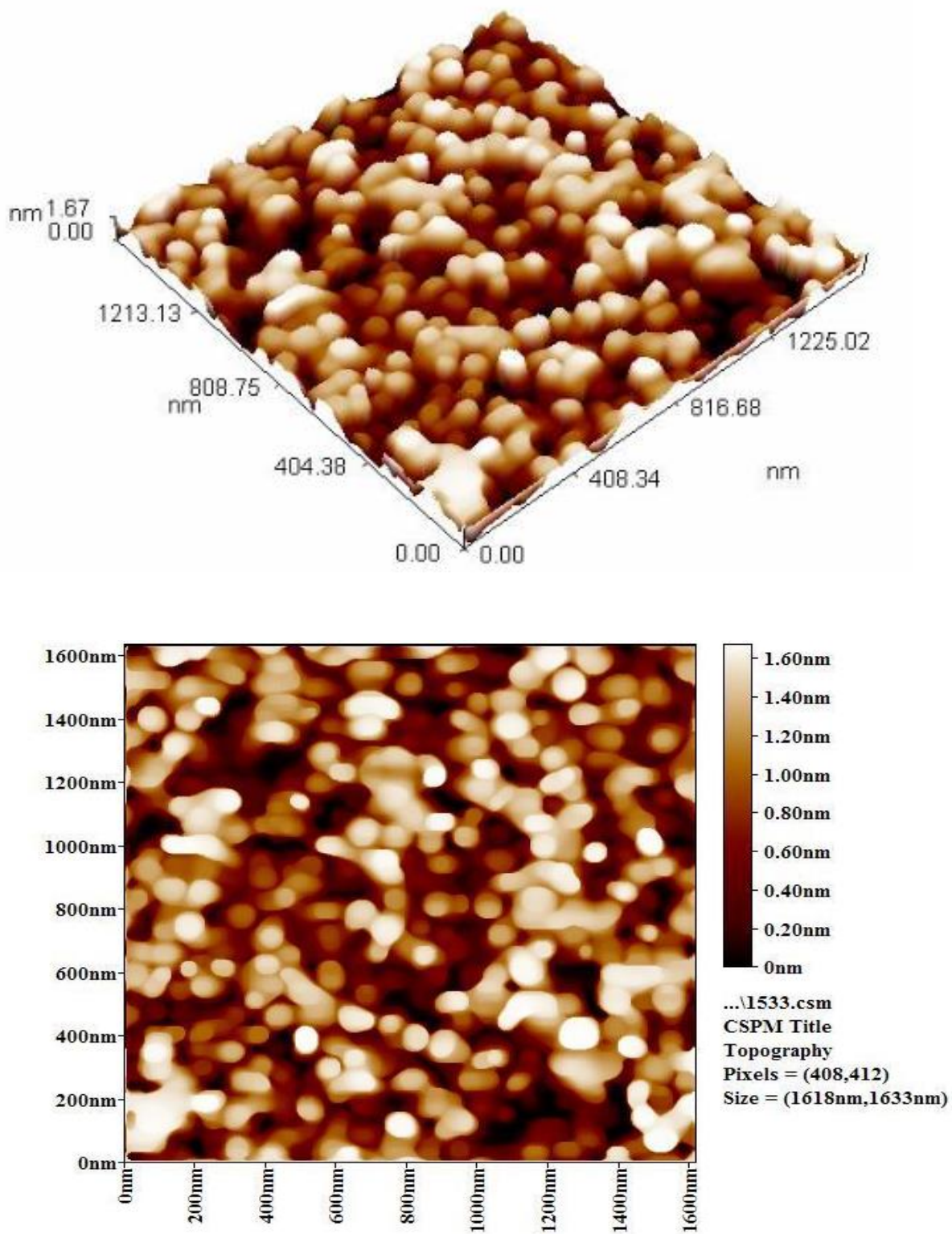


Figure 7. Two and Three dimension AFM Image for AlPO₄-5 (sample 9).

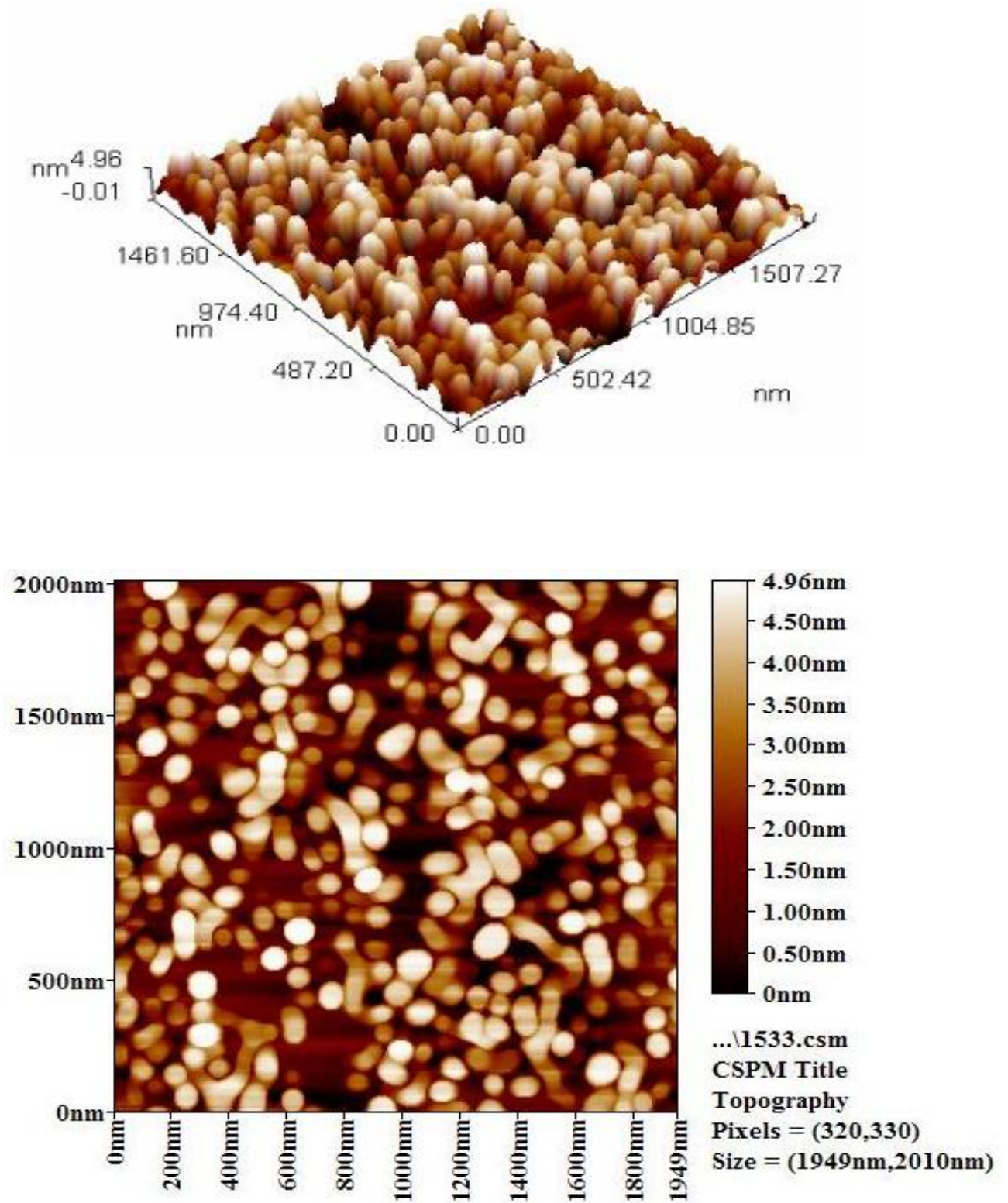


Figure 8. Two and Three dimension AFM Image for AlPO₄-5 (sample 11).

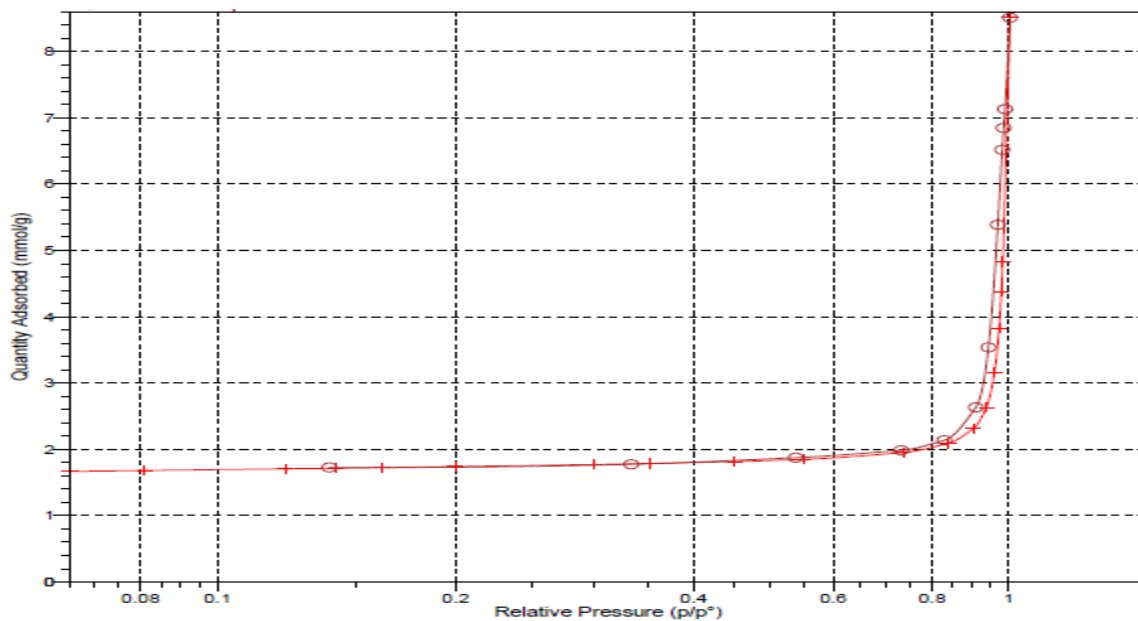


Figure 9. Isotherm Plot for AlPO₄-5 (M9).

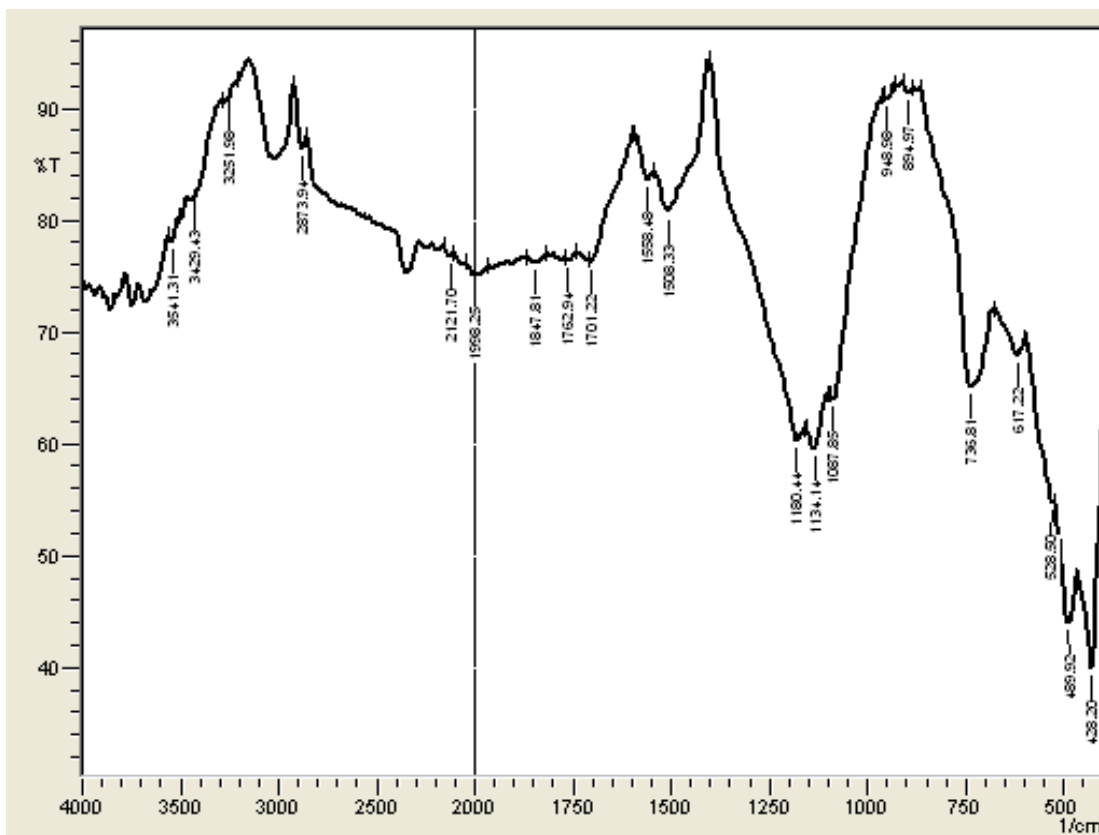


Figure 10. FTIR spectrum for AlPO₄-5.



Table 4. Types of bands in FTIR spectrum.

Type of Band	Wave length, cm^{-1}
T-O-T Asymmetric stretching	1160, 1130, 1087
T-O-T Symmetric stretching	736.8
T-O-T Bending	439 with shoulder at 489

T is either Al or P

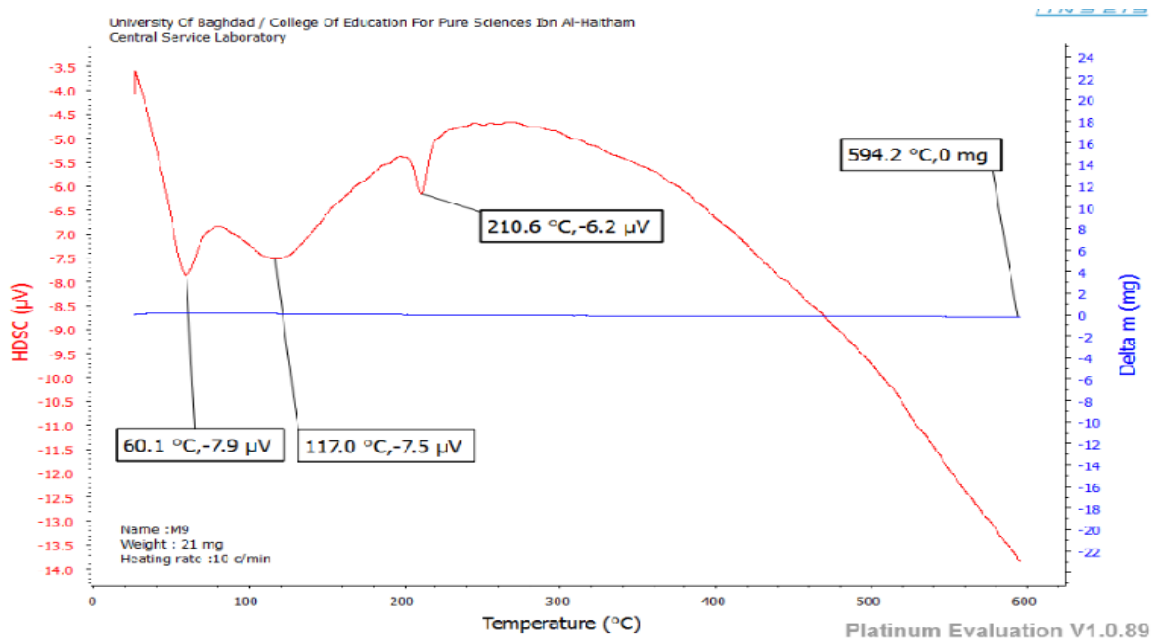


Figure 11. DSC-TGA for AlPO_4 (M9).